Sliding-PD Control Performance on Autonomous Underwater Gliders

Isabel Andrade-Bustos[1], Luis G. García-Valdovinos
and Tomás Salgado-Jiménez
Energy Division
Center of Engineering and Industrial Development (CIDESI)
Santiago de Querétaro, México
[1]Email: ibustos@cidesi.edu.mx

Manuel Bandala-Sánchez
Applied Electronics Division
Center of Engineering and Industrial Development (CIDESI)
Email: mbandala@cidesi.edu.mx

***Abstract*—The response of the ROGUE underwater glider controlled by a scheme called Sliding PD control is shown and described. This control law has been widely used in robot manipulators, quadrotors and underwater ROV's. This is a model-free and chattering-free controller that makes motion robust to disturbance and uncertainty. The ROGUE dynamic model calculated on the vertical plane take into account a ballast tank fixed at the buoyancy center, a movable mass capable of motion just along the longitudinal axis and eliminates the offset static point mass. These considerations simplify significantly the equations of motion. Through simulation results this nonlinear controller demonstrates that it ensures a steady glide by directly controlling the movable mass position along with the ballast mass.**

I. Introduction

The concept of an underwater robot, i.e. a gliding robot, capable of transforming vertical motion into horizontal as a consequence of a buoyancy force and small displacements of its internal masses was presented by Henry Stommel in 1989 [1]. This idea proposed the opportunity of underwater exploration for longer periods and lower cost, and also opened the window to a new and complex system, interesting for control experts and scientists. This concept has motivated the development of several operational gliders, including the SLOCUM [2], the Spray [3] and the Seaglider [4].

All existing gliders work by using the same principle, a variable mass with fixed position in order to change the buoyancy force and a fixed mass with variable position to change the vehicle's center of gravity, and therefore, the pitch angle. Fixed wings that helps to create a gliding performance, and isolation of moving parts from the sea environment.

Since an underwater glider has no thrusters or any other propulsion system (i.e. conventional motors) power consumption decrease notably compared to vehicles such as AUV's and ROV's. In order to start diving, an underwater glider changes its net buoyancy through the value of the variable mass (ballast tank), and changes the movable mass position in order to change its center of gravity and starts to glide using its wings. In that way it is possible to achieve mission endurances even for months.

Nowadays, gliders execute missions with conventional proportional-integral-derivative (PID) control loops [5] or using this type of controllers combined with dead band and saturation modules [6]. Here is presented a description of the dynamic model of the academic underwater glider ROGUE simplified to the vertical plane [7] and its response under a Sliding-PD controller [8]- [9] based on second order sliding modes. This nonlinear controller does neither require the dynamic model nor the parameters. Moreover, thanks to the second order sliding mode condition, attained since the beginning, the harmful chattering effect is totally removed, making the controller a suitable choice to be implement in real underwater gliders. This paper shows several simulations that creates high expectations for this controller applied on autonomous underwater gliders.

Additionally, a trajectory interpolation algorithm has been implemented in order to create a smooth transition between the initial and the final angle target. This algorithm generates several points through the trajectory, as a consequence the control signal increases or decreases slowly, therefore it helps to keep a precise tracking, save energy and increase the vehicle's autonomy.

II. ROGUE Dynamic Model

First of all, a defined nomenclature for the variables used is presented in table I. Some of them are defined for a three-dimensional motion, in spite of this analysis is restricted to the vertical plane those variables are necessary to define its interesting components.

This paper considers the equations of motion presented in [6]. These equations have been restricted to the vertical plane. The underwater glider ROGUE was modeled as a rigid body with a moving mass actuator ($\overline{m}$) and a variable ballast actuator (m_b). $\overline{m}$ is a fixed mass with variable position and m_b is a variable mass with fixed position. The translational velocity and angular velocity of the glider in body coordinates are $\mathbf{v} = [v_1 \quad v_2 \quad v_3]^T$ and $\boldsymbol{\Omega} = [\Omega_1 \quad \Omega_2 \quad \Omega_3]^T$, respectively. The mass matrix and the inertia matrix of the body-fluid system are $\mathbf{M} = diag(m_1 \quad m_2 \quad m_3)^T$ and $\mathbf{J} = diag(J_1 \quad J_2 \quad J_3)^T$, respectively. The position of the moving mass in the body frame is $\mathbf{r_p} = [r_{p1} \quad r_{p2} \quad r_{p3}]^T$.

978-0-933957-43-5 ©2015 MTS

TABLE I. VARIABLES DESCRIPTION

Name	Description
α	angle of attack,$\cos\alpha = v_1/\sqrt{v_1{}^2+v_3{}^2}$
$\mathbf{b}$	vehicle position vector from inertial frame
CB	center of buoyancy and origin of body frame
CG	center of gravity
D	drag force
$\mathbf{J_f}$	added inertia matrix
$\mathbf{J_s}$	inertia of stationary mass
$\mathbf{J}$	$J_f + J_s$
J_i	ith diagonal element of J
L	lift force
$\mathbf{M}$	sum of body and added mass
$\mathbf{M_f}$	added mass matrix
M_{DL}	viscous moment
m	mass of displaced fluid
$\bar{m}$	movable point mass
m_b	variable ballast mass located at CB
m_{fi}	ith diagonal element of M_f
m_i	ith diagonal element of M
m_h	uniformly distributed hull mass
m_s	stationary body mass, $m_s = m_h + m_w + m_b$
m_v	total vehicle mass, $m_v = m_s + \bar{m}$
m_w	point mass for nonuniform hull mass distribution
m_0	excess mass,$m_0 = m_v - m$
$\boldsymbol{\Omega}$	angular velocity in body coordinates
Ω_i	ith component of Ω
$\mathbf{P}$	total linear momentum in body coordinates
$\mathbf{P_p}$	linear momentum of $\bar{m}$ in body coordinates
$\mathbf{p}$	total linear momentum in inertial coordinates
$\mathbf{p_P}$	linear momentum of $\bar{m}$ in inertial coordinates
$\mathbf{R}$	rotation matrix for vehicle orientation
$\mathbf{r_p}$	position of movable mass $\bar{m}$ in body coordinates
r_{pi}	ith component of r_p
$\mathbf{r_w}$	position vector from CB to m_w
θ	pitch angle
$\bar{\mathbf{u}}$	$(u_1\ u_2\ u_3)^T$, force on sliding point mass
$\mathbf{u}$	$(u_1\ u_2\ u_3\ u_4)^T$, vector of control inputs
u_4	controlled variable mass rate, $u_4 = \dot{m}_b$
$\mathbf{V}$	speed in vertical plane, $V = \sqrt{(v_i{}^2 + v_3{}^2)}$
$\mathbf{V_d}$	desired speed in vertical plane
$\mathbf{v}$	velocity in body coordinates
v_i	ith component of v
x, y, z	components of vehicle position vector b
ξ	glide path angle, $\xi = \theta - \alpha$
ξ_d	desired glide path angle

A. Equations of Motion in the Vertical Plane

A corrected model of the ROGUE glider is presented in the vertical plane, the $\mathbf{i} - \mathbf{k}$ plane in inertial coordinates and the $\mathbf{e_1} - \mathbf{e_3}$ in the body coordinates. It is known,

$$\mathbf{R} = \begin{pmatrix} \cos\theta & 0 & \sin\theta \\ 0 & 1 & 0 \\ -\sin\theta & 0 & \cos\theta \end{pmatrix};\quad \mathbf{b} = \begin{pmatrix} x \\ 0 \\ z \end{pmatrix}$$

$$\mathbf{v} = \begin{pmatrix} v_1 \\ 0 \\ v_3 \end{pmatrix};\quad \boldsymbol{\Omega} = \begin{pmatrix} 0 \\ \Omega_2 \\ 0 \end{pmatrix};\quad \mathbf{r_p} = \begin{pmatrix} r_{p1} \\ 0 \\ r_{p3} \end{pmatrix}$$

$$\mathbf{P_p} = \begin{pmatrix} P_{p1} \\ 0 \\ P_{p3} \end{pmatrix};\quad \bar{\mathbf{u}} = \begin{pmatrix} u_1 \\ 0 \\ u_3 \end{pmatrix};$$

The following equations of motion represent the nonlinear dynamic model of underwater glider ROGUE:

$$\dot{x} = v_1\cos\theta + v_3\sin\theta \tag{1}$$

$$\dot{z} = v_3\sin\theta - v_1\cos\theta \tag{2}$$

$$\dot{\theta} = \Omega_2 \tag{3}$$

$$\begin{aligned}\dot{\Omega}_2 = \frac{1}{a}(&\overline{m}r_{p1}(P_{p1}\Omega_2 - L\cos\alpha - D\sin\alpha \\ &+\overline{m}\Omega_2\dot{r}_{p1} + m_1\Omega_2 v_1) - (m_3+\overline{m}) \\ &-(r_{p3}u_1 + P_{p1}\Omega_2 r_{p1} + v_1 v_3(m_1 - m_3) \\ &+g\overline{m}(r_{p1}\cos\theta + r_{p3}\sin\theta) + \overline{m}\Omega_2 r_{p1}\dot{r}_{p1} \\ &+\overline{m}\Omega_2 r_{p3} v_3 - \overline{m}(\Omega_2{}^2) r_{p1} r_{p3} \\ &-M_{DL}) + g m_0\cos\theta)\end{aligned} \tag{4}$$

$$\begin{aligned}\dot{v}_1 = \frac{1}{m_1}(&-m_3 v_3\Omega_2 - m_0 g\sin\theta + L\sin\alpha - u_1 \\ &-P_{p3}\Omega_2 - D\cos\alpha)\end{aligned} \tag{5}$$

$$\begin{aligned}\dot{v}_3 = \frac{1}{a}(&(\overline{m}r_{p1}{}^2 + J_2)(P_{p1}\Omega_2 - L\cos\alpha - D\sin\alpha \\ &+g m_0\cos\theta + \overline{m}\Omega_2\dot{r}_{p1} + m_1\Omega_2 v_1) \\ &-\overline{m}r_{p1}(r_{p3}u_1 - MDL + P_{p1}\Omega_2 r_{p1} \\ &+v_1 v_3(m_1 - m_3) + g\overline{m}(r_{p1}\cos\theta \\ &+r_{p3}\sin\theta) + \overline{m}\Omega_2 r_{p1}\dot{r}_{p1} + \overline{m}\Omega_2 r_{p3} v_3 \\ &-\overline{m}\Omega_2{}^2 r_{p1} r_{p3}))\end{aligned} \tag{6}$$

$$\dot{r}_{p1} = \frac{P_{p1}}{\overline{m}} - \Omega_2 r_{p3} - v_1 \tag{7}$$

$$\dot{r}_{p3} = \frac{P_{p3}}{\overline{m}} + \Omega_2 r_{p1} - v_3 \tag{8}$$

$$\dot{P}_{p1} = u_1 \tag{9}$$

$$\dot{P}_{p3} = u_3 \tag{10}$$

$$\dot{m}_b = u_4 \tag{11}$$

$$a = m_3\overline{m}r_{p1}{}^2 + J_2 m_3 + J_2\overline{m} \tag{12}$$

The hydrodynamic forces and moment are expressed in [6] as:

$$D = \frac{1}{2}\rho C_D(\alpha)AV^2 \approx (K_{D0} + K_D\alpha^2)(v_1{}^2 + v_3{}^2)$$

$$L = \frac{1}{2}\rho C_L(\alpha)AV^2 \approx (K_{L0} + K_L\alpha)(v_1{}^2 + v_3{}^2)$$

$$M_{DL} = \frac{1}{2}\rho C_M(\alpha)AV^2 \approx (K_{M0} + K_M\alpha)(v_1{}^2 + v_3{}^2)$$

Where $K's$ are constant hydrodynamic parameters.

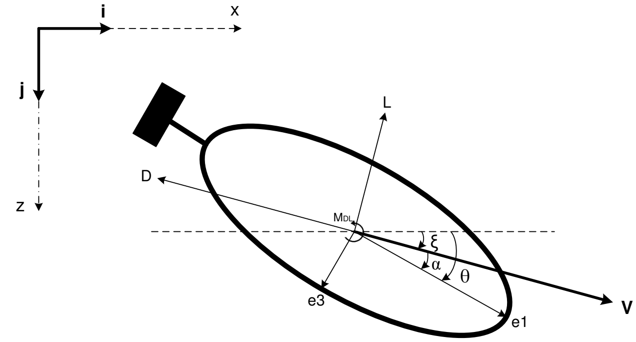

Fig. 1. Lift, Drag and Viscous Moment.

ROGUE is an academic underwater glider with the movable mass ($\bar{m}$) restricted to move only over the longitudinal axis (e_1). This means that r_{p3} is fixed, hence $\dot{r}_{p3} = 0$ and finally (8) becomes

$$P_{p3} = \bar{m}(v_3 - r_{p1}\Omega_2) \tag{13}$$

The new equations of motion are (1) to (11) excluding (8) and (10). Further, P_{p3} is replaced by (13) and u_3 is replaced by (10) which is computed by differentiating (13) with respect to time. In particular, (4) and (6) are replaced with

$$\begin{bmatrix} \dot{\Omega}_2 \\ \dot{v}_3 \end{bmatrix} = Z^{-1} \begin{bmatrix} \frac{1}{J_2}(f_1 - r_{p1}\bar{m}\Omega_2\dot{r}_{p1}) \\ \frac{1}{m_3}(f_2 - \bar{m}\Omega_2\dot{r}_{p1}) \end{bmatrix}$$

where

$$\begin{aligned} f_1 &= (m_3 - m_1)v_1v_3 - \bar{m}g(r_{p1}\cos\theta + r_{p3}\sin\theta) \\ &\quad + M_{DL} - r_{p3}u_1 - r_{p1}P_{p1}\Omega_2 - r_{p3}\bar{m}v_3\Omega_2 \\ &\quad + r_{p3}\bar{m}r_{p1}{\Omega_2}^2 \\ f_2 &= m_1v_1\Omega_2 + P_{p1}\Omega_2 + m_0g\cos\theta - L\cos\alpha - D\sin\alpha \\ &\quad + \bar{m}\dot{r}_{p1}\Omega_2 \\ Z &= \begin{bmatrix} 1 + \frac{\bar{m}{r^2}_{p1}}{J_2} & -\frac{\bar{m}r_{p1}}{J_2} \\ -\frac{\bar{m}r_{p1}}{m_3} & 1 + \frac{\bar{m}}{m_3} \end{bmatrix} \end{aligned}$$

III. CONTROLLER DESIGN

Based on [7] and modifying the original equations, a simulator of the academic underwater glider ROGUE has been developed. This is a MIMO, non-linear, underactuated, and strongly coupled system. Linear control laws based on local linearization exhibit a good performance when close to the gliding equilibrium.

A Sliding PD controller is considered a non-linear control scheme that yields to semiglobal stability of all closed-loop signals with exponential convergence of tracking errors.

Movable mass position (r_{p1}) and the variable mass value (m_b) are the output variables, and using a standard nomenclature we have:

$$\mathbf{q} = \begin{bmatrix} q_1 \\ q_2 \end{bmatrix} = \begin{bmatrix} r_{p1} \\ m_b \end{bmatrix} \tag{14}$$

The control outputs have been defined as $\mathbf{u} = [u_1 \quad u_2]^T$, where u_1 and u_2 are the control inputs of the glider. Now according with [8]- [9] we have:

$$u_i = -K_{di}S_{ri} \tag{15}$$

$$S_{ri} = S_{q_i} + K_i \int sgn(S_{q_i}) \tag{16}$$

$$S_{q_i} = S_i - S_i(t_0)exp^{-\kappa t} \tag{17}$$

$$S_i = (\dot{q}_i - \dot{q}_{id}) + \lambda_i(q_i - q_{id}) \tag{18}$$

where K_d, K, λ and $\kappa \in \mathbb{R}$ positives control constants.

Tuning the parameters is not obvious and special attention is paid to avoid misleading conclusion. Several simulation were carried out in order to induce the sliding surface for one of the variables (r_{p1}), once this objective was reached the same gains were used for the second variable (m_b). Values of the control parameters are shown in Table II.

TABLE II. FEEDBACK GAINS.

Par	K_d	λ	K	κ
Value	120	0.8	3	5

This control scheme has been applied during the first transition, changing the glide path angle from 0 to -30 degrees as a result of the displacement of the movable mass and the value of the variable mass, producing a nose down motion and the first pitch moment. Also, this controller was applied to produce and control the first cycle in a sawtooth pattern trajectory, in order to demonstrate that it is able to cope with the most critical point, i.e change the pitch angle from nose down to nose up and vice versa, this results will be shown in section IV.

IV. SIMULATION RESULTS

In order to validate the performance of the above-mentioned control scheme, several simulations were carried out. The ROGUE model parameters have been taken from [7] and are shown in table III:

TABLE III. PARAMETER VALUES OF THE ROGUE GLIDER

Parameter	Value	Unit
m	11.22	kg
$\bar{m}$	2	kg
m_0	± 0.36	kg
m_h	8.22	kg
m_1	2	kg
m_3	14	kg
J_2	0.1	Nm^2
r_{p3}	0.04	m
K_D	109	Ns/m^2
K_{D0}	18	Ns/m^2
K_L	306	Ns/m^2
K_{L0}	0	Ns/m^2
K_M	-36.5	Ns/m^2
K_{M0}	0	Ns/m^2

First of all, a glide path angle (ξ), a desired depth to start the transition from nose down to nose up (z_d) and a desired velocity (V_d) were selected, ($\xi_d = \pm 30$ $[degrees]$, $z_d = 4$ $[m]$ and $V_d = 0.3$ $[m/s]$). The ROGUE model has been solved, and is possible to compute values for r_{p1} and m_b that satisfy the desired conditions.

A sawtooth pattern is composed by cycles, and when we talk about gliders we say that each cycle is given by five stages: equilibrium-nose down, nose down-steady glide, critical transition, nose up-steady glide and nose up-equilibrium. A complete cycle was simulated and is shown in Fig. 7.

These five stages are easy to identify in Fig. 2, because changes in the movable mass position and the ballast rate impact directly over the glide path angle, i.e. the vehicle's trajectory. From zero to five seconds the equilibrium-nose down stage was presented, from five to thirty seconds a steady glide path was performed, it is possible to observe the critical transition during the next ten seconds, the fourth stage is presented during the next twenty five seconds and finally, the glider return to equilibrium during the last ten seconds of simulation.

Three different interpolated trajectories has been programmed in order to create the first sawtooth cycle. The first was a smooth profile from the initial condition ($r_{p1} = 0\ [m]$ and $m_b = 1\ [kg]$) to a desired value ($r_{p1} = 0.0041\ [m]$ and $m_b = 1.36\ [kg]$), a second one for the critical transition ($r_{p1} = 0.00041\ [m]$ and $m_b = 1.36\ [kg]$) to ($r_{p1} = -0.0041\ [m]$ and $m_b = 0.64\ [kg]$) and a final interpolation to reach equilibrium again, with values ($r_{p1} = -0.0041\ [m]$ and $m_b = 0.64\ [kg]$) to ($r_{p1} = 0\ [m]$ and $m_b = 1\ [kg]$). Worth to notice is that neutral buoyancy is achieved when $r_{p1} = 0\ [m]$ and $m_b = 1\ [kg]$.

Several graphics were computed and analyzed during simulation runs but only the most important are presented and discussed here. Fig. 2 shows the response of the controlled variables, there is possible to observe the accurate performance of the tracking, the real variables (r_{p1} and m_b) follow perfectly the desired trajectory.

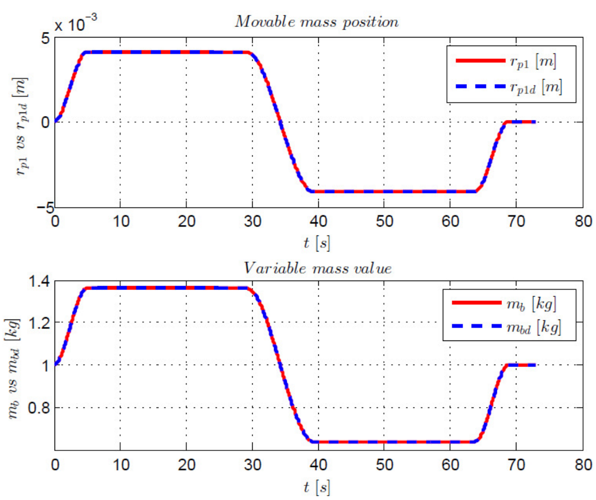

Fig. 2. Output responses of movable mass position and variable mass value.

A desired speed of the movable mass $(\dot{r_{p1}})$ and a desired rate of the variable mass $(\dot{m_b})$ were defined using a trajectory interpolation. Parameters of timing were the same for both variables, that's why in Fig. 2 and Fig. 3 their response look alike, but with different limits.

In Fig. 4 it is possible to observe the behavior of control signals over the interesting variables, u_1 represents the force exerted on the movable mass ($\bar{m}$) and u_4 is the control over the quantity of liquid inside the ballast tank (m_b). In section 2 we defined the mass rate of the ballast as a control input, and we can see how this has been accomplished by observe and compare these two variables in Fig. 3 and Fig. 4.

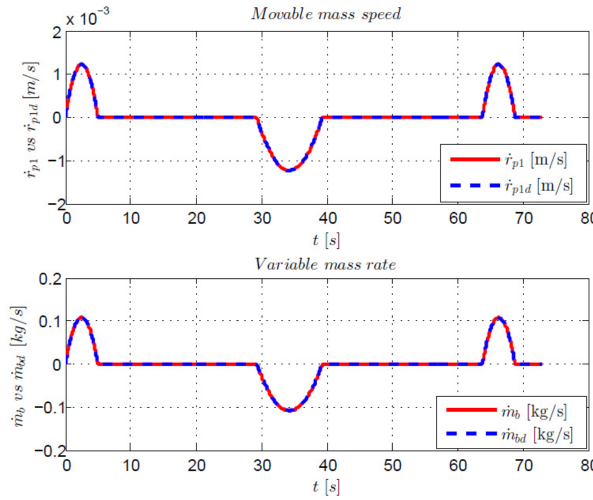

Fig. 3. Output responses of movable mass speed and variable mass rate.

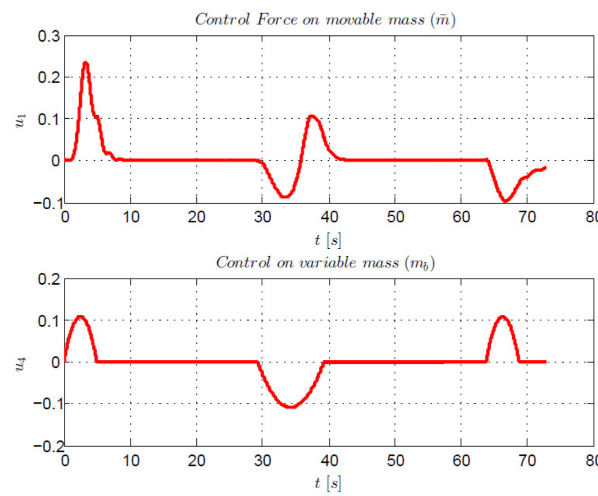

Fig. 4. Control signals.

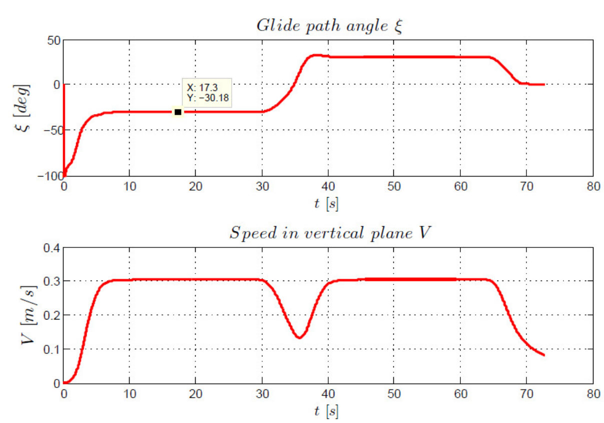

Fig. 5. Glide path angle and velocity behaviour in the vertical plane.

As it was mentioned, the glide path, pitch angle and velocity are consequence of changes in the generalized coordinates (r_{p1} and m_b), see Fig 5 and Fig. 6. During the first five seconds, these changes, in the next two seconds appears a small oscillation on both angles, then the desired values were reached.

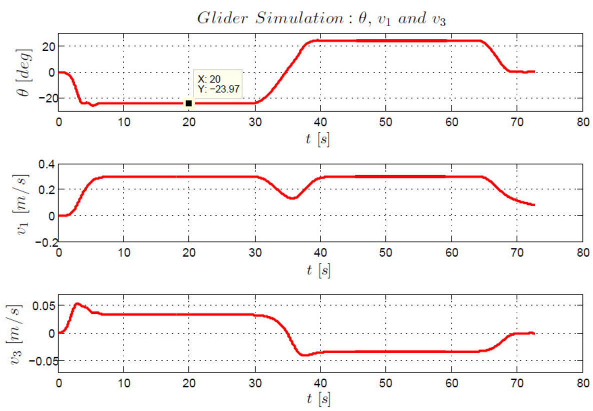

Fig. 6. Pitch angle and velocity components behaviour in the vertical plane.

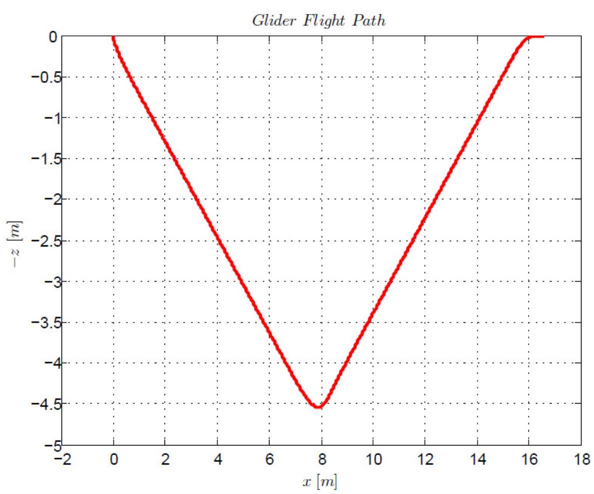

Fig. 7. Glide path on the vertical plane of ROGUE with the proposed control law.

The most important result for this work is to determine if a desired glide path and velocity could be reached through a PD Sliding, in Fig. 5 we demonstrate that this objective was accomplished with a negligible error. In Fig. 6 is shown the behaviour of θ (worth to remember that $\xi = \theta - \alpha$) , and the components of V.

Finally Fig. 7 shows the glide path on the vertical plane in the predicted sawtooth pattern. This results validate the effectiveness of the PD Sliding controller on a complex system such as an underwater glider.

V. Conclusion

A model free nonlinear controller applied on the ROGUE glider has been proposed obtaining very good simulation results. Nowadays legacy gliders use linear controllers as conventional PD or PID schemes. An underwater glider is a complex system, by nature it is unpredictable due to its high nonlinearity. The presented approach shows a controller able to cope with all these characteristics with excellent tracking performance. Trajectory interpolation algorithm contributes to the energy saving, due the outputs has not a sharp transition, this means a glider with limited power storage has a longer range and higher endurance.Based on the simulation results, it is proved that a Sliding-PD scheme is capable to control and reach a steady glide path for the ROGUE glider. Experimental results will be reported in a future paper.

VI. Acknowledgments

The authors would like to thank CONACYT support under a master scholarship No. 302060. This work was partially supported by CONACYT, Mexico, by the grants: PDCPN2013-01-0215770 and CONACYT-SENER-Hidrocarburos-2012-01.

References

[1] H. Stommel,"The slocum mission",Oceanography, vol. 2, no, 1, pp. 22-25, 1989.

[2] D. C. Webb. P. J. Simonetti, and C. P. Jones. "Slocum: An underwater glider propelled by environmental energy", IEEE Journal of Oceanic Engineering, vol, 26, no 4, pp. 447-452, 2001.

[3] J. Sherman, R. Davis, W. Owens, J. Valdes, "The autonomous underwater glider spray," IEEE, Journal of Oceanic Engineering, vol. 26, no. 4, pp. 437-446, 2001.

[4] C. C. Eriksen, T. J Osse. R. D. Light,T. Wen, T. W. Lehman, P. L. Sabin, J. W. Ballard, and A. M. Chiodi, "Seaglider: A long-range autonomous underwater vehicle for oceanographic research", IEEE, Journal of Oceanic Engineering, vol. 26, no. 4, pp. 424-436, 2001.

[5] P. Bhatta and N. E. Leonard, "Stabilization and coordination of underwater gliders", Proceedings of the 41st IEEE conference on decision and control, IEEE Press, Dec.2002, pp. 2081-2086.

[6] J. G. Graver, Underwater gliders: Dynamics, control and design. PhD Thesis, Princeton University, May 2005.

[7] N. E. Leonard and J. G. Graver, "Model-based feedback control of autonomous underwater gliders", IEEE Journal of Oceanic Engineering, vol. 26, no. 4, pp. 633-645, 2001.

[8] L. G. García-Valdovinos, T. Salgado-Jiménez, "On the Dynamic Positioning Control of Underwater Vehicles subject to Ocean Currents", IEEE CCE 2011, pp. 361-366, Mérida, Mexico, 2011

[9] L.G. García-Valdovinos, T. Salgado-Jiménez, M. Bandala-Sánchez, L. Nava-Balzanzar, R. Hernández-Alvarado and J.A. Cruz-Ledesma, "Modeling, Design, and Robust Control of a Remotely Operated Underwater Vehicle", International Journal of Advanced Robotic Systems, Vol. 11, No. 1, pp. 1-16, January 2014. ISSN: 1729-8806

[10] Spong, Mark W and Hutchinson, Seth and Vidyasagar, Mathukumalli, Robot modeling and control, Wiley New York, vol. 3, 2006.